ChemComm

COMMUNICATION

View Article Online
View Journal | View Issue

Cite this: *Chem. Commun.*, 2026, **62**, 4851

Received 21st November 2025,
Accepted 2nd February 2026

DOI: 10.1039/d5cc06620d

rsc.li/chemcomm

Dual pharmacokinetic modifier strategy for synergistically enhanced tumor accumulation of PSMA-targeting radioligand

Takuma Hasegawa, † Kazuma Nakashima, † Hiroyuki Watanabe and Masahiro Ono *

Herein, we report a novel molecular design strategy that introduces two distinct pharmacokinetic modifiers into a single radioligand to achieve the synergistic enhancement of tumor accumulation. We newly designed a small-molecule-based radioligand, which contains both a positively charged unit and an albumin binder, and demonstrated its enhanced tumor accumulation.

Radiopharmaceuticals, drugs that incorporate radionuclides for diagnostic or therapeutic applications, have attracted marked attention as a novel modality for cancer treatment.[1,2] In general, radiopharmaceuticals include carriers for delivery to cancerous regions. Various types of carriers have been reported; in particular, small molecules have been frequently selected due to their high tumor penetration and rapid clearance from non-target organs.[3]

Prostate cancer is one of the most common malignancies in males worldwide, requiring early detection and an established method of therapy.[4] On the surface of prostate cancer cells, prostate-specific membrane antigen (PSMA) is highly expressed, and its expression level correlates with the malignancy of prostate cancer.[5,6] Therefore, PSMA is recognized as an attractive target of prostate cancer, and so many small-molecule-based radioligands targeting it have been developed.[6,7] Recently, Pluvicto® ([^{177}Lu]Lu-PSMA-617) was approved by the U.S. Food and Drug Administration (FDA) and European Medicines Agency (EMA) for the treatment of patients with metastatic castration-resistant prostate cancer.[8] As a result of promising outcomes on administering Pluvicto® in clinical settings, PSMA-617 is now regarded as the current gold standard among PSMA-targeting ligands.[9] However, some patients with prostate cancer do not respond to treatment using Pluvicto® due to insufficient accumulation of radionuclides in cancerous regions.[10] Consequently, enhancing tumor accumulation of PSMA-617 is considered a promising strategy to improve therapeutic efficacy for patients with prostate cancer.

To address this challenge, the introduction of pharmacokinetic modifiers, chemical structures that enhance the tumor accumulation of radioligands, has been widely adopted.[11–14] Through this approach, we previously developed potent PSMA-targeting radioligands, [^{111}In]In/[^{225}Ac]Ac-PDI2 (Fig. 1A).[15] [^{111}In]In/[^{225}Ac]Ac-PDI2 was designed by incorporating the positively charged diethylenetriamine (DETA) structure, identified during our exploration of poly(ethylenimine) (PEI) structures, as a pharmacokinetic modifier into PSMA-617. The purpose of introducing the DETA structure was to enhance the tumor-residualizing properties of PSMA-617 by increasing electrostatic repulsion against lysosomal membranes.[16] [^{111}In]In-PDI2 exhibited enhanced tumor-residualizing properties *in vitro* and *in vivo* through introduction of the DETA structure compared with [^{111}In]In-PSMA-617. As a result, [^{111}In]In-PDI2 could be used to visualize PSMA-expressing tumors with higher contrast, and [^{225}Ac]Ac-PDI2 demonstrated

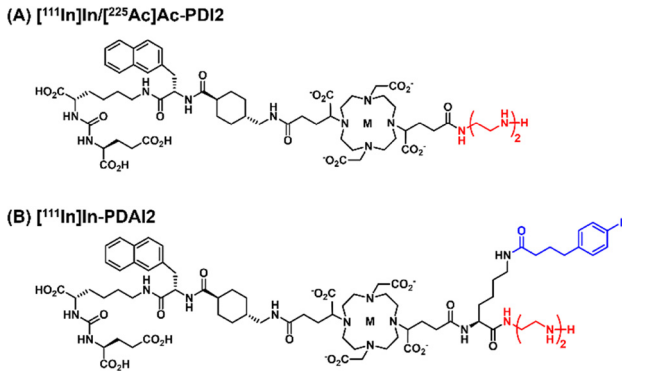

Fig. 1 Chemical structures of (A) [^{111}In]In/[^{225}Ac]Ac-PDI2 and (B) [^{111}In]In-PDAI2. DETA and IPBA structures are highlighted in red and blue, respectively. M means radiometal ($^{111}In^{3+}$ or $^{225}Ac^{3+}$).

Department of Patho-Functional Bioanalysis, Graduate School of Pharmaceutical Sciences, Kyoto University, 46-29 Yoshida Shimoadachi-cho, Sakyo-ku, Kyoto 606-8501, Japan. E-mail: ono@pharm.kyoto-u.ac.jp
† These authors contributed equally to this work.

greater antitumor effects than [^{111}In]In/[^{225}Ac]Ac-PSMA-617 without the DETA structure. However, the maximal tumor accumulation of [^{111}In]In-PDI2 was comparable with that of [^{111}In]In-PSMA-617. Therefore, it is considered that increasing the efficiency of [^{111}In]In-PDI2 delivered into the tumor leads to further improvement of its tumor accumulation.

To improve the efficiency for delivering small-molecule-based radioligands to tumors, we focused on albumin binders (ALBs) as pharmacokinetic modifiers. ALBs non-covalently interact with albumin in plasma, resulting in prolonged blood half-lives and enhanced tumor accumulation of radioligands.[17,18] Regarding PSMA-targeting radioligands, it has been demonstrated that the introduction of 4-(*p*-iodophenyl)butyric acid (IPBA) derivatives as ALBs enhances their tumor accumulation.[19–22] Therefore, we hypothesized that introducing an IPBA structure into [^{111}In]In-PDI2 would prolong its blood half-life and increase the amount of radioligands delivered to tumors, resulting in further enhanced tumor accumulation through the synergistic effects of DETA and IPBA structures.

In this study, we designed a novel PSMA-targeting ligand, PDAI2 (Fig. 1B), which utilizes the dual pharmacokinetic modifier strategy to achieve synergistic enhancement of tumor accumulation. PDAI2 is composed of four units: a PSMA-targeting ligand as a carrier for delivery to cancerous regions, 1,4,7,10-tetraazacyclododecane-1,4,7,10-tetraacetic acid (DOTA) structure as a radiometal chelator, DETA structure as a positively charged unit, and an IPBA structure as ALB. To evaluate the rationality of our molecular design strategy, we synthesized [^{111}In]In-PDAI2 and assessed its biological properties. ^{111}In was selected due to its sufficiently long half-life of 2.8 days for assessment of [^{111}In]In-PDAI2 *in vivo*.

The synthetic routes of [^{nat}In]In-PDAI2 are detailed in Schemes S1–S4. DETA, IPBA, and DOTA structures were conjugated sequentially using Lys as a linker, resulting in the formation of a DOTA-IPBA-DETA moiety. PDAI2 was synthesized *via* solid-phase peptide synthesis (SPPS), involving the condensation of the DOTA-IPBA-DETA moiety and PSMA-targeting ligand on resin, and a subsequent deprotection reaction of *t*Bu and Boc protecting groups, with a marked purity of >95% (Fig. S1). ^{111}In-labeling was performed by incubating the precursor with [^{111}In]$InCl_3$ in acetate buffer (Scheme 1). After completion of the chelating reaction, [^{111}In]In-PDAI2 was obtained with a radiochemical yield of 72.3% and purity of >95% (Fig. S2). In the HPLC chromatogram of $^{nat/111}$In-labeled PDAI2, two distinct peaks were observed. This is likely due to the isomerization caused by differences in metal coordination with the DOTA chelator, and similar phenomena were frequently reported in previous studies.[23–25]

To evaluate the overall charge of [^{111}In]In-PDAI2, a cellulose acetate electrophoresis (CAE) assay was performed (Fig. S3). [^{111}In]In-PDAI2 and [^{111}In]In-PDI2 migrated to the anode side, and similar migration distances were observed for both ^{111}In-labeled ligands. This result indicates that the insertion of IPBA does not modify the electrostatic properties of [^{111}In]In-PDAI2 in respect to [^{111}In]In-PDI2.

A cell saturation binding assay using PSMA-expressing LNCaP cells was performed to assess the binding affinity of [^{111}In]In-PDAI2 for PSMA (Fig. 2A). [^{111}In]In-PDAI2 exhibited specific binding to LNCaP cells with a K_d value of 18.2 nM. The binding affinity of [^{111}In]In-PDAI2 for LNCaP cells was comparable with that of [^{111}In]In-PDI2 with a K_d value of 22.8 nM, suggesting that the addition of an IPBA structure to [^{111}In]In-PDI2 does not significantly affect the PSMA-binding property.[15]

To evaluate the relative albumin-binding potencies of [^{111}In]In-PDAI2 and [^{111}In]In-PDI2, an albumin-binding assay by the ultrafiltration method using human serum albumin (HSA) was performed according to our previous report (Fig. 2B).[26] After incubating ^{111}In-labeled radioligands in HSA solutions at increasing concentrations, the percentage of the high-molecule-weight fraction (albumin-bound fraction) was calculated. As the concentration of HSA increased, the albumin-bound fraction of [^{111}In]In-PDAI2 also increased. Moreover, the albumin-bound fractions of [^{111}In]In-PDAI2 were significantly larger than those of [^{111}In]In-PDI2 without an IPBA structure, suggesting that the introduction of an IPBA structure enhances binding to albumin. This result indicated that the IPBA structure in [^{111}In]In-PDAI2 functioned effectively as ALB. Regarding the result for [^{111}In]In-PDI2, an increase in the albumin-bound fraction was also observed at higher concentrations of HSA. This may be due to the interactions between a 2-naphthyl group within the PSMA-targeting ligand structure and hydrophobic cavity of albumin.[27]

To assess the cellular retention properties of [^{111}In]In-PDAI2, cell internalization and efflux assays using LNCaP cells were performed (Fig. 3 and Tables S1, S2). In the cell internalization assay, ^{111}In-labeled radioligands were incubated for 0 h, 1 h, 2 h, and 4 h after binding to PSMA on the surface of LNCaP cells,

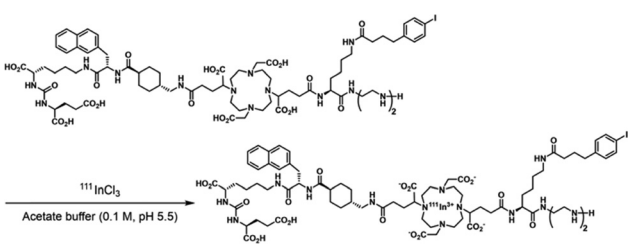

Scheme 1 ^{111}In-labeling of PDAI2.

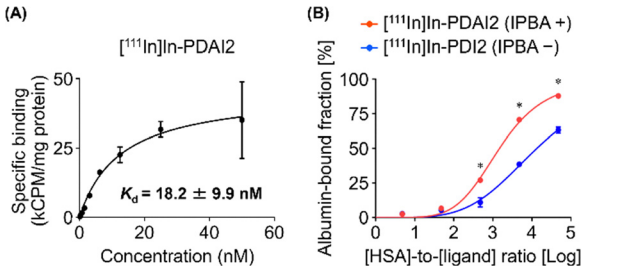

Fig. 2 (A) The specific binding of [^{111}In]In-PDAI2 in the presence of PDAI2 to LNCaP cells in the cell saturation binding assay. CPM means counts per minute. (B) Albumin-binding curves of [^{111}In]In-PDAI2 (red) and [^{111}In]In-PDI2 (blue) using HSA. *P < 0.05 (two-way analysis of variance (ANOVA) with *post hoc* Bonferroni's test).

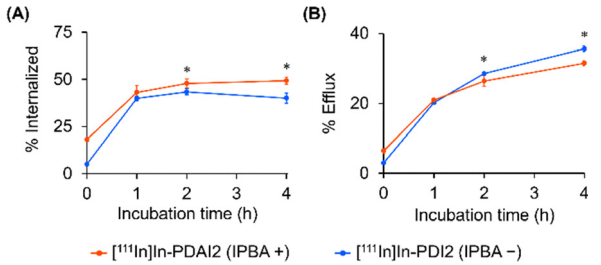

Fig. 3 Internalization (A) and efflux (B) assays of [^{111}In]In-PDAI2 (red) and [^{111}In]In-PDI2 (blue) using LNCaP cells. *$P < 0.05$ (two-way ANOVA with *post hoc* Bonferroni's test).

and radioactivity in the internalized fractions, which contain radioligands internalized into cells, was determined (Section S8, SI). [^{111}In]In-PDAI2 was rapidly internalized after starting the incubation, and its radioactivity in the internalized fraction was higher than that of [^{111}In]In-PDI2 at and after 2 h postincubation. In the same fashion, effluxes of ^{111}In-labeled radioligands were monitored for 0 h, 1 h, 2 h, and 4 h after internalization into LNCaP cells, and the radioactivity in the efflux fractions, which contain released radioligands from LNCaP cells, was determined. Although time-dependent efflux of [^{111}In]In-PDAI2 from LNCaP cells was observed after the start of incubation, [^{111}In]In-PDAI2 exhibited lower radioactivity in the efflux fraction at and after 2 h postincubation than [^{111}In]In-PDI2. Based on the findings of cell internalization and efflux assays, introduction of the IPBA structure as ALB does not adversely affect, and may even enhance, internalization and/or residualizing properties of [^{111}In]In-PDI2. While the underlying mechanism remains unclear, these results raise the possibility that presence of the IPBA structure positively influences membrane interactions and/or alters subcellular trafficking pathways of PSMA-targeting radioligands.

The pharmacokinetic properties of [^{111}In]In-PDAI2 were evaluated by performing a biodistribution study using LNCaP tumor-bearing mice, and the results were compared with those of [^{111}In]In-PDI2 (Fig. 4 and Tables S3–S5).[15] [^{111}In]In-PDAI2 exhibited significantly higher-level blood retention (16.05% and 5.48% injected dose (ID)/g at 4 h and 24 h postinjection, respectively) compared with those of [^{111}In]In-PDI2 (0.58% and 0.12% ID/g, respectively). These results suggested that introduction of the IPBA structure prolonged the blood half-life of [^{111}In]In-PDAI2.

Regarding tumor accumulation, levels of [^{111}In]In-PDAI2 (40.86%, 99.53%, and 73.59% ID/g at 4 h, 24 h, and 96 h postinjection, respectively) were markedly higher than those of [^{111}In]In-PDI2 (20.74%, 25.47% and 13.54% ID/g, respectively). These results indicate that introduction of an IPBA structure efficiently enhanced tumor accumulation of [^{111}In]In-PDI2.

Among healthy organs, the kidney is known to express PSMA; therefore, higher-level renal uptake of [^{111}In]In-PDAI2 (89.23%, 74.56%, and 15.68% ID/g at 4 h, 24 h, and 96 h postinjection, respectively) was observed compared with other normal organs.[28,29] [^{111}In]In-PDAI2 showed markedly higher renal uptake than [^{111}In]In-PDI2 (52.31%, 4.85%, and 1.21% ID/g at 4 h, 24 h, and 96 h postinjection, respectively), and the significant difference was observed at 24 h postinjection. This is likely due to the increased blood residence time of delivery of [^{111}In]In-PDAI2 to the kidney as a result of the higher radioactivity remaining in the blood achieved by introduction of the IPBA structure.

To assess the specific binding of [^{111}In]In-PDAI2 to PSMA, an *in vivo* blocking study was performed (Fig. S4 and Table S6). Regardless of the co-injection of a PSMA-inhibitor, nearly equal amounts of [^{111}In]In-PDAI2 in the blood were observed at 4 h postinjection. However, tumor accumulation and renal uptake of [^{111}In]In-PDAI2 were significantly decreased (14.41% and 9.03% ID/g, respectively) on co-injection of the PSMA-inhibitor. These results suggest the *in vivo* specificity of [^{111}In]In-PDAI2 for the PSMA-expressing tumor.

In conclusion, we designed and synthesized a novel PSMA-targeting radioligand, [^{111}In]In-PDAI2, which contains both DETA and IPBA structures as pharmacokinetic modifiers. Regarding *in vitro* experiments, [^{111}In]In-PDAI2 exhibited

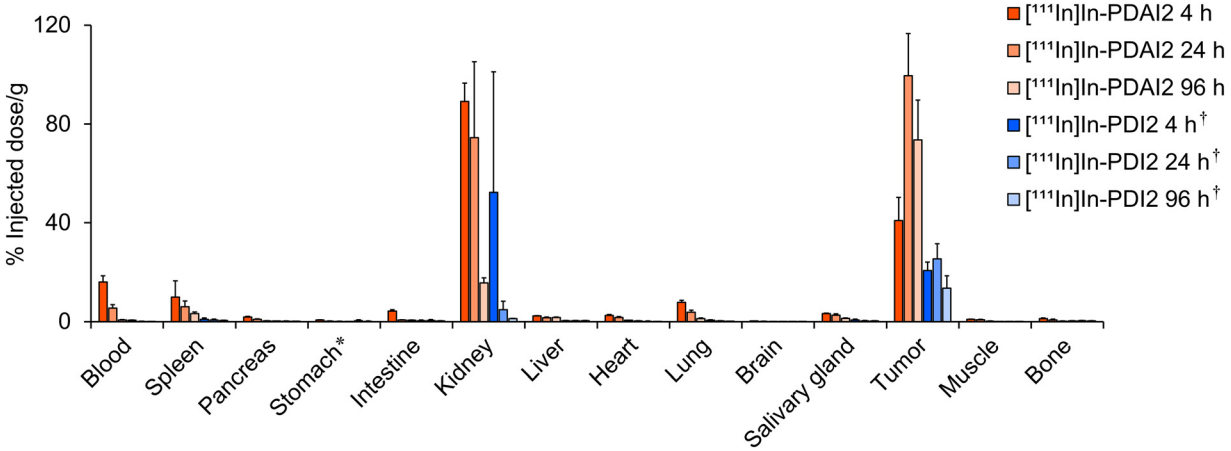

Fig. 4 Biodistribution of radioactivity among organs and tissues after the intravenous injection of [^{111}In]In-PDAI2 (red) and [^{111}In]In-PDI2 (blue) into LNCaP tumor-bearing mice. *Values are expressed as % injected dose. †Data on [^{111}In]In-PDI2 were reproduced with permission from ref. 15, Copyright 2025 American Chemical Society.

anticipated charge characteristics, preserved binding affinity for PSMA, marked binding to albumin, and improved residualizing properties in tumor cells. In the biodistribution study, prolonged blood half-lives and enhanced tumor accumulation of [^{111}In]In-PDAI2 were observed. These findings support our dual pharmacokinetic modifier strategy as an effective approach for achieving synergistic enhancement of tumor accumulation of PSMA-targeting radioligands. To translate our dual pharmacokinetic modifier strategy to therapeutic applications, a biodistribution study and an evaluation of therapeutic efficacy will be performed using PDAI2 labeled with therapeutic radiometals (*e.g.*, ^{177}Lu and ^{225}Ac) in future investigations. Moreover, our molecular design strategy is not limited to a PSMA-targeting ligand, but can also be applied to radioligands targeting other cancer biomarkers. Based on these findings, we anticipate that the molecular design strategy demonstrated in this study will contribute significantly to the future development of next-generation radiopharmaceuticals.

This work was financially supported by AMED under Grant numbers: JP23ama221604, JP24ama221604, and JP25ama221604.

Conflicts of interest

There are no conflicts to declare.

Data availability

The data supporting this article have been included as part of supplementary information (SI). Supplementary information: synthetic procedures, characterization data, experimental details, HPLC chromatograms, results of CAE assay, cell internalization assay, cell efflux assay, biodistribution study, and *in vivo* blocking study of ^{111}In-labeled radioligands. See DOI: https://doi.org/10.1039/d5cc06620d.

References

1 G. Sgouros, L. Bodei, M. R. McDevitt and J. R. Nedrow, *Nat. Rev. Drug Discovery*, 2020, **19**, 589–608.
2 K. Vermeulen, M. Vandamme, G. Bormans and F. Cleeren, *Semin. Nucl. Med.*, 2019, **49**, 339–356.
3 T. Zhang, H. Lei, X. Chen, Z. Dou, B. Yu, W. Su, W. Wang, X. Jin, T. Katsube, B. Wang, H. Zhang, Q. Li and C. Di, *Cell Death Discovery*, 2024, **10**, 16.
4 N. S. Wagle, L. Nogueira, T. P. Devasia, A. B. Mariotto, K. R. Yabroff, F. Islami, A. Jemal, R. Alteri, P. A. Ganz and R. L. Siegel, *CA Cancer J. Clin.*, 2025, **75**, 308–340.
5 J. S. Horoszewicz, E. Kawinski and G. P. Murphy, *Anticancer Res.*, 1987, **7**, 927–935.
6 T. Wüstemann, U. Haberkorn, J. Babich and W. Mier, *Med. Res. Rev.*, 2019, **39**, 40–69.
7 A. P. Kozikowski and J. Neale, *J. Med. Chem.*, 2025, **68**, 20972–20978.
8 L. M. Unterrainer, J. Calais and N. H. Bander, *Annu. Rev. Med.*, 2024, **75**, 49–66.
9 O. Sartor, J. de Bono, K. N. Chi, K. Fizazi, K. Herrmann, K. Rahbar, S. T. Tagawa, L. T. Nordquist, N. Vaishampayan, G. El-Haddad, C. H. Park, T. M. Beer, A. Armour, W. J. Perez-Contreras, M. DeSilvio, E. Kpamegan, G. Gericke, R. A. Messmann, M. J. Morris, B. J. Krause and V. Investigators, *N. Engl. J. Med.*, 2021, **385**, 1091–1103.
10 M. Straub, J. Kupferschläger, L. M. Serna Higuita, M. Weissinger, H. Dittmann, C. la Fougère and F. Fiz, *J. Nucl. Med.*, 2023, **64**, 1431–1438.
11 Z. Huangfu, J. Yang, J. Sun, B. Xu, L. Tao, J. Wu, F. Wang, G. Wang, F. Meng and Z. Zhong, *J. Controlled Release*, 2024, **375**, 767–775.
12 J. F. Santos, M. T. Braz, P. Raposinho, F. Cleeren, I. Cassells, S. Leekens, C. Cawthorne, F. Mendes, C. Fernandes and A. Paulo, *Mol. Pharmaceutics*, 2024, **21**, 216–233.
13 X. Y. Cui, Z. Li, Z. Kong, Y. Liu, H. Meng, Z. Wen, C. Wang, J. Chen, M. Xu, Y. Li, J. Gao, W. Zhu, Z. Hao, L. Huo, S. Liu, Z. Yang and Z. Liu, *Nature*, 2024, **630**, 206–213.
14 L. M. Deberle, M. Benešová, C. A. Umbricht, F. Borgna, M. Büchler, K. Zhernosekov, R. Schibli and C. Müller, *Theranostics*, 2020, **10**, 1678–1693.
15 T. Hasegawa, K. Nakashima, Y. Tarumizu, M. Tada, Y. Maya, H. Watanabe and M. Ono, *J. Med. Chem.*, 2025, **68**, 10190–10202.
16 K. Nakashima, H. Watanabe and M. Ono, *J. Med. Chem.*, 2023, **66**, 12812–12827.
17 Y. Tao, V. Jakobsson, X. Chen and J. Zhang, *Acc. Chem. Res.*, 2023, **56**, 2403–2415.
18 L. Meng, J. Fang, X. Lin, R. Zhuang, L. Huang, Y. Li, X. Zhang and Z. Guo, *J. Controlled Release*, 2025, **382**, 113757.
19 S. Iikuni, Y. Tarumizu, K. Nakashima, Y. Higaki, H. Ichikawa, H. Watanabe and M. Ono, *J. Med. Chem.*, 2021, **64**, 13429–13438.
20 S. Tsuchihashi, K. Nakashima, Y. Tarumizu, H. Ichikawa, H. Jinda, H. Watanabe and M. Ono, *J. Med. Chem.*, 2023, **66**, 8043–8053.
21 C. A. Umbricht, M. Benešová, R. Schibli and C. Müller, *Mol. Pharmaceutics*, 2018, **15**, 2297–2306.
22 F. Reissig, K. Zarschler, Z. Novy, M. Petrik, K. Bendova, D. Kurfurstova, J. Bouchal, M. C. Ludik, F. Brandt, K. Kopka, M. Khoylou, H. J. Pietzsch, M. Hajduch and C. Mamat, *Theranostics*, 2022, **12**, 7203–7215.
23 S. Tsuchihashi, K. Nakashima, H. Watanabe and M. Ono, *ACS Med. Chem. Lett.*, 2025, **16**, 797–803.
24 J. Schlesinger, I. Koezle, R. Bergmann, S. Tamburini, C. Bolzati, F. Tisato, B. Noll, S. Klussmann, S. Vonhoff, F. Wuest, H. J. Pietzsch and J. Steinbach, *Bioconjugate Chem.*, 2008, **19**, 928–939.
25 H. Suzuki, M. Araki, K. Tatsugi, K. Ichinohe, T. Uehara and Y. Arano, *J. Med. Chem.*, 2023, **66**, 8600–8613.
26 N. Kazuta, K. Nakashima, H. Watanabe and M. Ono, *ACS Pharmacol. Transl. Sci.*, 2024, **7**, 2401–2413.
27 Y. Liu, M. Chen, G. Bian, J. Liu and L. Song, *J. Biochem. Mol. Toxicol.*, 2011, **25**, 362–368.
28 D. J. Bacich, J. T. Pinto, W. P. Tong and W. D. Heston, *Mamm. Genome*, 2001, **12**, 117–123.
29 Z. Lee, W. D. Heston, X. Wang and J. P. Basilion, *Eur. J. Nucl. Med. Mol. Imaging*, 2023, **50**, 2944–2946.

